# Detection of foreign body using fast thermoacoustic tomography with a multielement linear transducer array

Liming Nie, Da Xing,[a] Diwu Yang, Lvming Zeng, and Quan Zhou
*MOE Key Laboratory of Laser Life Science, South China Normal University, Guangzhou 510631, China and Institute of Laser Life Science, South China Normal University, Guangzhou 510631, China*

(Received 5 December 2006; accepted 30 March 2007; published online 26 April 2007)

Current imaging modalities face challenges in clinical applications due to limitations in resolution or contrast. Microwave-induced thermoacoustic imaging may provide a complementary modality for medical imaging, particularly for detecting foreign objects due to their different absorption of electromagnetic radiation at specific frequencies. A thermoacoustic tomography system with a multielement linear transducer array was developed and used to detect foreign objects in tissue. Radiography and thermoacoustic images of objects with different electromagnetic properties, including glass, sand, and iron, were compared. The authors' results demonstrate that thermoacoustic imaging has the potential to become a fast method for surgical localization of occult foreign objects. © *2007 American Institute of Physics*. [DOI: 10.1063/1.2732824]

Significant progress has been made in the past several years in photoacoustic imaging. Microwave-induced thermoacoustic imaging which shares similar principles with photoacoustic imaging could potentially combine the advantages of microwave imaging and ultrasound imaging, to achieve high resolution and high absorption contrast.[1–5] Moreover, microwave-induced thermoacoustic imaging may provide wider medical applications because microwave radiation has higher tissue penetration depth than light and also has different contrast mechanisms. This feature of thermoacoustic imaging can be employed to detect occult foreign bodies in tissue.

Thermoacoustic signal generation is a result of microwave-induced thermal effect. A small temperature surge can be produced when a biological tissue is irradiated by a microwave pulse of adequate energy. Subsequently, the heated structure thermally expands and contracts, becoming a source of acoustic wave. By detecting the sound wave and via signal reconstruction, thermoacoustic tomography (TAT) can be realized based on the differences in microwave absorption inside the target.

Accidental invasion of foreign body into human tissue is rather frequent, especially in the case of a traumatic or iatrogenic injury. The common methods for locating foreign bodies present several drawbacks: Radiography is invasive and not ideal for detecting nonradiopaque substances such as glass and wood while magnetic resonance imaging (MRI) cannot function when metals are involved. And computed tomography and MRI are both cumbersome and expensive. TAT, which relies on microwave absorption, can help visualize electromagnetic differences in biological tissue. It has the potential to become an effective and low-cost biomedical imaging modality for disease diagnose. Furthermore, it could be used to recognize and locate foreign bodies rapidly and accurately.

We have developed a fast photoacoustic imaging system using multielement linear transducer array.[6–9] A microwave-induced thermoacoustic tomography prototype was also designed and developed.[10] In this study, this system was applied to detect and localize occult foreign bodies in biological tissues. A phase-controlled focus technique is used to reduce data acquisition time and a limited-field-filtered back-projection algorithm is used to enhance spatial resolution.[8] In addition, a full-view filtered back-projection reconstruction algorithm and a circular scanning geometry for acquiring more signals at different angles are adopted.

The experimental set up is shown in Fig. 1, where a laboratory coordinate system $(X, Y, Z)$ is also depicted for reference. The microwave pulses, obtained with a 1.2 G microwave generator (BW-1200HPT, China), have a pulse duration of 0.5 $\mu$s. The microwave pulses were coupled into a rectangular waveguide with a cross section of $127\times63$ mm$^2$, the microwave pulses irradiated a sample uniformly with an energy density of 0.4 mJ/cm$^2$. The sample was placed on a rotary sample stage and immersed in a polyvinyl chloride tank, which was filled with transformer oil for better coupling of acoustic waves.

A B-mode system (model CTS-200, SIUI, China) was employed as the platform with 320 vertical transducer elements (EZU-PL21, SIUI, China), which have a midfrequency of 3.5 MHz, a nominal bandwidth of 65%, and a sensibility of approximately 1 mV/Pa. The transducer with a

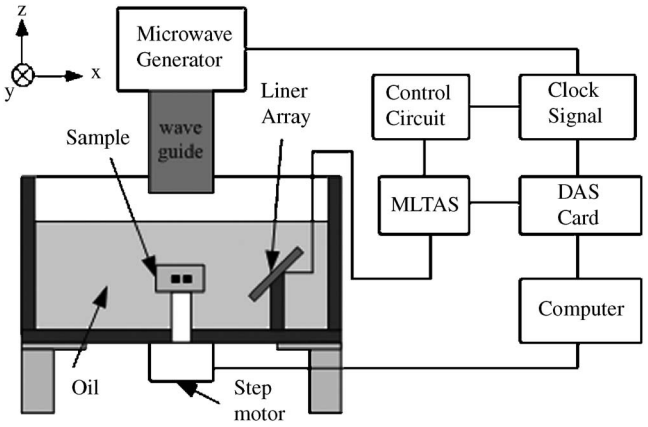


FIG. 1. Schematic of the experimental setup for microwave-induced thermoacoustic data acquisition system.

[a]Author to whom correspondence should be addressed; FAX: +86-20-85216052; electronic mail: xingda@scnu.edu.cn

 

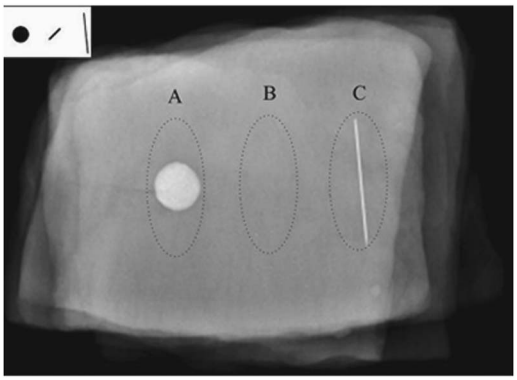


FIG. 2. X-ray images of different samples, sand, glass bar, and iron needle corresponding to positions A, B, and C, embedded in pork fatty tissue. (Inset: the schematic cross section of the samples' placement.)

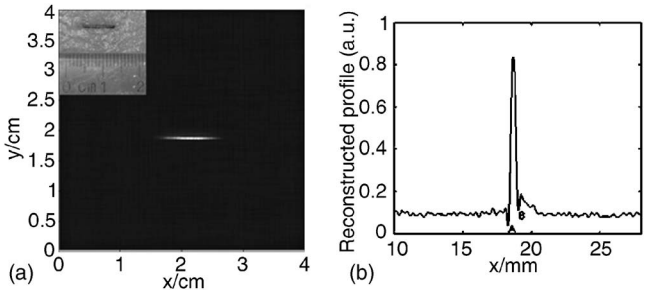


FIG. 3. (a) Reconstructed thermoacoustic image of the glass bar under 1 cm pork muscle tissue. (Inset: cross section of the glass bar embedded in pork muscle tissue.) (b) Normalized line profile of the reconstructed image shown in Fig. 3(a) with $x=22$ mm.

scanning width of 102 mm can be divided into 64 subgroups, and each subgroup consists of five transducer elements, which have a length of 10 mm, a width of 0.3 mm, a pitch of 0.04 mm, and a thickness of 0.5 mm. A two-channel data acquisition system (DAS) card (Compuscope 12100, Gage Applied Co., Montreal, Quebec, Canada) was used to record thermoacoustic signals which were then transferred to a personal computer. The card features a high-speed 12 bit analog-to-digital converter with a sampling rate of 100 MHz.

A custom-built control circuit provided a synchronized signal to trigger the microwave generator and the DAS card. With the multiway electronic switch of multielement linear transducer array system, the custom-built control circuit selected 11 transducer elements of the linear transducer array to capture the induced themoacoustic signals. The captured signals received by the transducer elements from the test sample, after preamplification and phase adjustment, were acquired with the DAS card without averaging, reducing the scanning time to 5 s at each scanning stop. The sample was rotated in the horizontal plane (*X*-*Y* plane) allowing the transducer to capture signals within limited detection views, which effectively eliminates the problem that the focused ultrasonic transducer can only receive finite signals from boundaries of tissues which are nearly perpendicular to the axis of the transducer. The system operation and data collection are controlled by the personal computer and more details about the system can be found in the references.[6–10]

To verify the applicability of x-ray detection of foreign bodies, four pieces of pork fatty tissue with arbitrary shapes were sequentially stacked up. A ball of sand, a glass bar, and an iron needle were embedded under three pieces of pork tissue, with the embedded objects being 7.3 cm from the x-ray illuminated tissue surface. The x-ray images of the embedded samples, shown in Fig. 2, were acquired using a Shimadzu 500 mA radiographic machine (Shimadzu, Japan), with exposure conditions of 60 kV and 3 mA. The sand and the iron needle are discernible in positions A and C, with excellent contrasts. However, the glass bar is unrecognizable (Fig. 2, position B), due to low physical density of glass. Hence it is unreliable to use x ray to detect foreign body of low density contrast with the surrounding tissue.[11]

For thermoacoustic imaging, a phantom of tissue-glass bar was constructed. A piece of homogeneous pork muscle tissue was cut and made into an arbitrary shape with a thickness of 2 cm. Then a small screwdriver was used to carefully make a straight slot to place the glass bar. The glass bar was dyed with ink to increase its photographic visibility. Finally, the glass bar was buried beneath another piece of pork muscle tissue with 1 cm thickness. The reconstructed thermoacoustic image of the phantom with the glass bar hidden in biological tissue is shown in Fig. 3, with the inset showing the actual picture and size of the sample. The image of Fig. 3(a) was subjected to thresholding in order to display only the highest bits of brightness, so that the resolution is improved at the cost of dynamic range of the contrast. The reconstructed image matches well with the actual phantom. Figure 3(b) shows the corresponding normalized line profile of the reconstructed image at position $x=22$ mm in Fig. 3(a). The resolution of the system is estimated to be about 0.5 mm [defined as the distance between points A and B in the line plot in Fig. 3(b)], according to the resolution criterion defined in the literature.[12]

In the next experiment, the round sand buried in the biological tissue was imagined. A piece of homogeneous chicken breast tissue was cut and made into an arbitrary shape. Then a small screwdriver was used to carefully carve a round pouch. Sand was placed in the pouch and the sample was covered by another piece of chicken breast tissue of 2 cm thickness. Thermoacoustic signals at 20 scanning stops around the sample were acquired to reconstruct the image. Figure 4 shows the reconstructed thermoacoustic image of the round sand phantom, with the cross section of the sample shown in the inset; the geometrical shape of the round sand is in good agreement with the real subject and its boundary is clearly resolved.

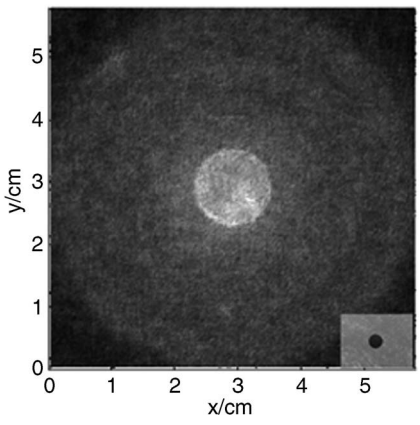


FIG. 4. Thermoacoustic image of round sand inside chicken breast tissue. The sand sample was buried 2 cm below the surface of the chicken tissue. (Inset: cross section of the round sand in chicken breast tissue.).

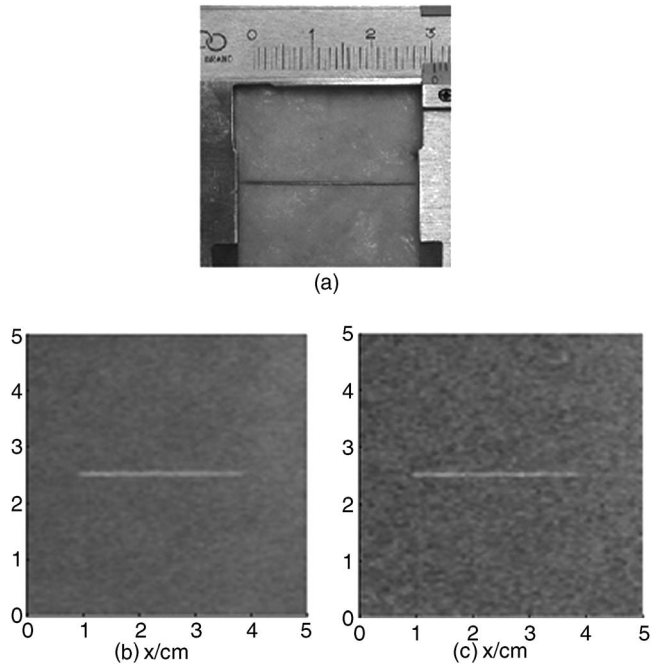


FIG. 5. (a) Cross section of a tissue sample with an iron needle embedded in pork fatty tissue. (b) Thermoacoustic image of the iron bar 5.3 cm below the tissue surface. (c) Thermoacoustic image of the iron needle 7.6 cm below the tissue surface.

An iron needle of diameter 0.5 mm and length 30 mm was embedded in pork fatty tissues of a rectangular shape and its transverse cross section is shown in Fig. 5(a). The tissue containing the embedded object was imaged with two pieces of pork tissue sequentially placed above the needle, making the embedded object 5.3 and 7.6 cm below the microwave illuminated tissue surface, respectively. The thermoacoustic images of the iron needles are shown in Figs. 5(b) and 5(c). At the depth of 5.3 cm, the image is a little blurred but the needle is easily discernible [Fig. 5(b)]. At the depth of 7.6 cm, the sound to noise ratio (SNR) noticeably deteriorated and the needle became obscure, yet still recognizable [Fig. 5(c)].

Along the microwave attenuation direction, the maximum imaging depth is affected by the microwave absorption and the noise level. At the frequency in our experiments, 1.2 GHz, the penetration depths for fat and muscle are 14 and 2.4 cm, respectively, and for normal breast tissue and malignant breast tissue 6.4 and 3.6 cm, respectively.[13] Most other soft have a penetration depth between those of muscle and fat. With the multielement phase-controlled focus technique, the SNR is high because the signals from a particular point outside the focal region could be canceled out after synthesizer and the signal intensity for each point of interest is the sum of the signals from transducers at many positions.

Our experimental results suggest that a sample with sufficiently different electromagnetic properties and embedded as much as 7.6 cm deep in biological tissue can be imaged using our thermoacoustic system. The studies have shown that TAT has the capacity to visualize foreign body with good contrast using a multielement linear transducer array. This application can be helpful in imaging glass and other objects in tissue not visible with x-ray radiography. In addition, this technique can be useful for studies in phantoms and *in vitro* tissues. We conclude that TAT has the potential to provide an effective, fast, and low-cost alternative method for imaging foreign objects in human and animals. For the microwave at the frequency of 1.2 GHz, the energy level used in our experiments is within the safety standard.[14]

This research is supported by the National Natural Science Foundation of China (60378043, 30470494, and 30627003) and the Natural Science Foundation of Guangdong Province (015012 and 2004B10401011).

[1]R. A. Kruger, K. K. Kepecky, A. M. Aisen, D. R. Reinecke, G. A. Kruger, and W. L. Kiser, Radiology **211**, 275 (1999).
[2]G. Ku and L. H. Wang, Med. Phys. **27**, 1195 (2000).
[3]X. Wang, Y. Pang, G. Ku, X. Xie, G. Stoica, and L.-H. V. Wang, Nat. Biotechnol. **21**, 803 (2003).
[4]R. O. Esenaliev, A. A. Karabutov, and A. A. Oraevsky, IEEE J. Sel. Top. Quantum Electron. **5**, 981 (1999).
[5]Y. Su, R. K. Wang, F. Zhang, and J. Q. Yao, Chin. Phys. Lett. **25**, 512 (2006).
[6]Y. G. Zeng, D. Xing, Y. Wang, B. Z. Yin, and Q. Chen, Opt. Lett. **29**, 1760 (2004).
[7]B. Z. Yin, D. Xing, Y. Wang, Y. G. Zeng, Y. Tan, and Q. Chen, Phys. Med. Biol. **49**, 1339 (2004).
[8]D. W. Yang, D. Xing, H. M. Gu, Y. Tan, and L. M. Zeng, Appl. Phys. Lett. **87**, 94101 (2005).
[9]D. W. Yang, D. Xing, Y. Tan, H. M. Gu, and S. H. Yang, Appl. Phys. Lett. **88**, 174101 (2006).
[10]L. M. Zeng, D. Xing, H. M. Gu, D. W. Yang, S. H. Yang, and L. Zh. Xiang, Chin. Phys. Lett. **23**, 1215 (2006).
[11]T. B. Hunter and M. S. Taljanovic, Radiographics **23**, 731 (2003).
[12]Y. Xu and L. H. V. Wang, IEEE Trans. Ultrason. Ferroelectr. Freq. Control **53**, 542 (2006).
[13]C. C. Johnson and A. W. Guy, Proc. IEEE **60**, 692 (1972).
[14]IEEE Standard for Safety Levels with Respect to Human Exposure to Radio Frequency Electromagnetic Fields 3 kHz to 300 GHz, IEEE Standard C95.1 (1999).